SUPPLEMENTAL MATERIALS FOR "REASSESSING THE FLOW LAW OF GLACIER ICE USING SATELLITE OBSERVATIONS"

Joanna D. Millstein[1*], **Brent M. Minchew**[2], **Samuel S. Pegler**[3]

[1]Massachusetts Institute of Technology - Woods Hole Oceanographic Institute Joint Program in Oceanography/Applied Ocean Science and Engineering, Cambridge, MA, USA
[2]Department of Earth, Atmospheric, and Planetary Sciences, Massachusetts Institute of Technology, Cambridge, MA, USA
[3]School of Mathematics, University of Leeds, Leeds, UK
[*]To whom correspondence should be addressed; E-mail: jdmill@mit.edu.

Preprint, compiled August 12, 2021

Constitutive Relationship of Ice Flow

The most commonly used constitutive relation, Glen's Flow Law (*1*), is semi-empirical as it is derived from simplified physical models, observations of natural ice flows such as borehole deformation measurements and ice flow velocities, and laboratory experiments on polycrystalline ice aggregates comparable to ice sheet conditions (*2–9*). Glen's is a power law rheology, which is useful in its simplicity to approximate the behavior of a non-Newtonian fluid by relating the strain rate and deviatoric stress. In the form proposed by Glen (*1*), the strain rate refers to the secondary (minimum) creep constrained on small, polycrstalline laboratory ice crystals. It has been shown, however, that the tertiary (steady-state) creep is perhaps a more appropriate measure of ice sheet flow for the anisotropic and high total strain accumulation of glacier ice (*10*). The convention of glaciological literature is to adopt $n = 3$, describing a shear-thinning viscous fluid. However, diverse experiments and observations have shown the exponent to range from $n = 1$ to integers as high as 11, implying various mechanisms of deformation (*4*, *11*).

In this work, we test and calibrate Glen's Flow Law for polycrystalline ice:

$$\dot{\epsilon}_e = A\tau_e^n, \tag{1}$$

where $\dot{\epsilon}_e$ is the effective strain rate, τ_e the effective deviatoric stress, n the stress exponent, and A the rate factor (*1*). In its most simplified form, A can be expressed as a function of temperature according to

$$A = A_0 \exp\left(-\frac{Q}{RT'}\right), \tag{2}$$

where A_0 is a constant factor, Q is the activation energy, R is the universal gas constant, and T' is the temperature difference to the pressure melting point (*12*, *13*). The effective strain rate and effective deviatoric stress are defined as the square root of the second invariant of the strain rate and deviatoric stress tensor, respectively, which is a measure of total magnitude (*14*). By definition these quantities are

$$\dot{\epsilon}_e^2 = \frac{1}{2}(\dot{\epsilon}_{xx}^2 + \dot{\epsilon}_{yy}^2 + \dot{\epsilon}_{zz}^2) + \dot{\epsilon}_{xy}^2 + \dot{\epsilon}_{xz}^2 + \dot{\epsilon}_{yz}^2, \tag{3}$$

$$\tau_e^2 = \frac{1}{2}(\tau_{xx}^2 + \tau_{yy}^2 + \tau_{zz}^2) + \tau_{xy}^2 + \tau_{xz}^2 + \tau_{yz}^2. \tag{4}$$

(*15*). Here, τ_{ij} is the deviatoric stress tensor, representative of changes in shape but not volume, and $\dot{\epsilon}_{ij}$ is the strain rate tensor, describing the rate of deformation of a material. The power law relationship shows the dependence of strain rate on applied stress and temperature, and typically uses least-squares regression to constrain the stress exponent from observations on natural ice masses (*3*, *16*, *17*) and laboratory experiments on isotropic polycrystalline ice (*1*, *4*, *8*, *18*). From these constraints, typical values for the constants have been inferred as $n = 3$, and for this value of n, the rate factor, A, is shown to exhibit a common range between $1.8 - 95 \times 10^{-25}$ s^{-1} Pa^{-n} dependent on the ice temperature, crystal size and orientation, and impurity concentration (*12*). It is worth noting that A is assumed to be a

scalar, although fully accounting for anisotropy in the crystallographic fabric of glacier ice would require representation of A with a second order tensor. In this work, our consideration of an extensional flow regime avoids this complication.

Glen's Flow Law assumes that ice is an incompressible polycrystalline structure deforming as a viscous fluid. Ice viscosity is non-linearly dependent on deviatoric stresses, which can be shown from the information in Equations 1, 3, and 4 where we can conclude:

$$2\eta\dot{\epsilon}_{ij} = \tau_{ij} \tag{5}$$

where η is the effective dynamic viscosity

$$\eta = \frac{1}{2A\tau_e^{n-1}} = \frac{1}{2A^{1/n}}\dot{\epsilon}_e^{\frac{1-n}{n}} \tag{6}$$

The stress (and strain rate) dependence of η shows that the viscosity of ice decreases with increasing stress, a characteristic often known as shear-thinning (or pseudoplastic) viscosity.

Field evaluations for the flow law exponent confront the problem of covariance of stress with other factors that influence the viscosity (*19*). Historically, laboratory experiments made the evaluations of the flow law from the minimum strain rate observed, which is a measure of secondary creep in ice and not unconditionally representative of larger strain observed in naturally flowing ice masses (*10*). Distinguishing the transition from a minimum strain rate to the tertiary creep in experimental studies reveals a shift in the value of the flow law exponent to a higher value, such as the work from Treverrow (*8*) where the minimum strain rates reveal $n = 3$ and the tertiary strain rates exhibit $n = 4$. For this reason, the mechanism of deformation in polycrystalline ice is critical for constraining the values of n and A, as the grain size and fabric have major influence over the viscosity alongside temperature and stress (*4*).

Solving for Effective Stress

Conservation of momentum (Stokes equations) describes all forces acting on the volume of glacier ice such that

$$\frac{\partial \tau_{ij}}{\partial x_j} - \frac{\partial p}{\partial x_i} - \rho g_i = 0 \tag{7}$$

where p is the pressure, ρg_i is the driving gravitational force (with $\boldsymbol{g} = g\hat{\boldsymbol{z}}$), and summation is implied for repeated indices. For a layer of ice floating on top of an ocean, we can derive depth-integrated equations to describe the balance of forces in such a system, given that the ice shelf is much larger in horizontal extent than in thickness (*20*). At scales of order the ice thickness, bending (and bridging) stresses are negligible, allowing us to simplify the equilibrium equations (*21*). As a result, we take the vertical normal stress to be hydrostatic, or equivalent to the overburden stress (weight of the ice per unit area). This can be expressed as

$$p = -\rho g z + \rho g' H + \tau_{zz} = -\rho g z + \rho g' H - \tau_{xx} - \tau_{yy} \tag{8}$$

where H is the ice thickness, $g' = g(\rho_w - \rho)/\rho_w$ is the reduced gravity, and the second equality arises from the fact that the deviatoric stress tensor is traceless as a consequence of the incompressiblity of ice. Eq. 8 is derived by integrating the vertical component of Eq. 7 and applying the condition of continuous normal stress at the top and bottom of the layer.

Then, neglecting basal drag (due to our focus on ice shelves) and depth integrating the x-component of Eq. 7, we can obtain

$$\frac{\partial}{\partial x}\left[H(2\tau_{xx} + \tau_{yy})\right] + \frac{\partial}{\partial y}(H\tau_{xy}) = \rho g' H \frac{\partial H}{\partial x}. \tag{9}$$

A complete derivation can be found in (*22*), which uses different notation but reveals the same outcome.

Our initial constraint to focus on areas with low shear strain rates allows us to eliminate the second term in Equation 9. Furthermore, we can assume that the lateral normal stresses (τ_{yy}) are small compared with the longitudinal normal stresses (τ_{xx}) due to our emphasis on areas with $\epsilon_{xx} \gg \epsilon_{yy}$. Vastly reduced, what began as four components - extension, lateral shear, basal drag, and buoyancy - now only requires terms for extension and buoyancy to illustrate the force balance of an unconfined ice shelf (*23*). Equation 9 is now

$$\frac{\partial}{\partial x}(2H\tau_{xx}) = \rho g' H \frac{\partial H}{\partial x}. \tag{10}$$

We can now rearrange the right-hand side of Equation 10 to an equivalent form

$$\frac{\partial}{\partial x}(2H\tau_{xx}) = \frac{1}{2}\rho g' \frac{\partial}{\partial x}(H^2). \tag{11}$$

Integrating this equation subject to the free stress condition at the front of the ice shelf and simplifying the resulting equation, we obtain

$$\tau_{xx} = \frac{1}{4}\rho g' H, \tag{12}$$

which we use as the basis for our analysis of extensional deviatoric stress in floating ice shelves. This derivation shows how we can use the extensional deviatoric stress as the total effective stress in our regions of interest, allowing us to use a dataset of ice thickness to determine the stress in the system parameter.

Generating Strain Rate Fields

The effective strain rate window size employed for the analysis has a recognized influence over the values for the rate factor and flow law. Spatial heterogeneity of the effective strain rate calculated using a Savitzy-Golay filter is smoothed and absorbed as the window sizes increase, and we choose to employ strain rates created with a window size of 31, which equates to 3720 m. We find that this is the best intermediary raster which represents distinct features, such as locally elevated strain rate at pinning points, while maintaining a smooth surface across a region along-flow on the ice shelf. To ensure that this window size is the most appropriate for our application, we use typical recommendations of length scales between 4-10 ice thicknesses (*12*, *24*). This recommendation originates from work used to minimize the errors, as represented by the sum of the square differences between the polynomial fit and the velocity fields, seeking a value that minimizes the misfit (*25*). The window size used preserves the values of strain rates in regions with low shear while removing artefacts from data collection of velocity fields and prominent surface features such as crevassing. In this way, we can use a visual assessment to determine the appropriate strain rate field. Importantly, the length scale used to calculate the gradients of the velocity field do not vary markedly in the regions appropriate for analysis in this study. We are using aggregates of cells with negligible shear stresses and small gradients across the ice thickness, so we expect areas with little noise (*26*).

Viable Areas for Analysis

The fast-flowing, extensional regions of Antarctic ice shelves can be identified by extracting grid cells in which the along-flow strain-rate and the effective strain-rate are sufficiently similar. Described in the main text, the ratio between the extensional strain rates $\dot{\epsilon}_{xx}$ and the horizontal effective strain rates $\dot{\epsilon}_e$ cannot exceed $\sqrt{2}$. We deem a criteria $\dot{\epsilon}_{xx} \geq \dot{\epsilon}_e$ to be the minimum acceptable value of similarity between the along-flow and effective strain rate, as this both highlights large, spatially congruous regions on ice shelves while excluding areas close to ice shelf margins and the grounding zone. Importantly, this criteria appropriately excludes regions undergoing complex flow where our intuition presumes dominant shear stresses and prominent lateral confinement. The full map is shown in Figure S1, with a few individual ice shelves in Figure S2. The appropriate area for analysis comprises 24.7% of all ice shelf area, clearly identifying large belts of grid cells where the ice if flowing in a nearly extensional regime. Moreover, many of these zones have small horizontal gradients in the ice thickness data, and avoid regions with known surface crevassing. This helps our analysis by removing regions with large jumps in strain rate between grid cells, leaving behind unexceptional portions of the ice shelf. The range of values for the stress and strain used for Figure 2 in the main text and Figure S3 below are shown in Figure S4, further illustrating this point.

Value of the Flow Law Rate Factor

Figure S3 shows values of the flow law rate factor, A, found from the same regions used for Figure 3 in the main text. While the values of n nearly resemble a normal distribution, with values hewing closer to $n = 4$, the values of A for the same areas reveal a very different behavior worth commenting on. Typically, the recommended base value of A is 3.5×10^{-25} Pa^{-3} s^{-1} for a temperature of $-10°$C and a flow law exponent $n = 3$. The value of A is influenced by the value of n as shown in the units of the term, and increasing n by a full integer value dramatically shifts the possible values of A. Notably, the range of stresses over each region are typically small, influencing the $y-$intercept in each regression created. Physical properties of the ice are different among each ice shelf, and the value of A has the ice temperature and activation energy explicitly wrapped up in the term. While the physical meaning of n is likely to do more with the stress-state of glacier ice, it is likely that A varies by other influences such as temperature and impurities that are not explicitly accounted for in this study.

References

1. J. W. Glen, *Proceedings of the Royal Society of London. Series A. Mathematical and Physical Sciences* **228**, 519–538 (1955).
2. R. B. Alley, *Journal of Glaciology* **38**, 245–256 (1992).
3. P. D. Bons *et al.*, *Geophysical Research Letters* **45**, 6542–6548 (2018).
4. D. Goldsby, D. L. Kohlstedt, *Journal of Geophysical Research: Solid Earth* **106**, 11017–11030 (2001).
5. R. Hooke, *Reviews of Geophysics* **19**, 664–672 (1981).

6. K. C. Jezek, R. B. Alley, R. H. Thomas, *Science* **227**, 1335–1337 (1985).
7. R. H. Thomas, *Journal of Glaciology* **12**, 55–70 (1973).
8. A. Treverrow, W. F. Budd, T. H. Jacka, R. C. Warner, *Journal of Glaciology* **58**, 301–314 (2012).
9. J. Weertman, *Annual Review of Earth and Planetary Sciences* **11**, 215–240 (1983).
10. W. Budd, T. Jacka, *Cold Regions Science and Technology* **16**, 107–144 (1989).
11. K. Cuffey, J. Kavanaugh, *Geology* **39**, 1027–1030 (2011).
12. K. M. Cuffey, W. S. B. Paterson, *The Physics of Glaciers* (Academic Press, 2010).
13. R. Greve, H. Blatter, *Dynamics of ice sheets and glaciers* (Springer Science & Business Media, 2009).
14. J. W. Glen, *IASH Publ* **47**, e183 (1958).
15. C. J. Van Der Veen, I. Whillans, *Journal of Glaciology* **36**, 324–339 (1990).
16. F. Gillet-Chaulet, R. C. Hindmarsh, H. F. Corr, E. C. King, A. Jenkins, *Geophysical Research Letters* **38** (2011).
17. E. C. Pettit, E. D. Waddington, *Journal of Glaciology* **49**, 359–369 (2003).
18. W. Durham, H. Heard, S. H. Kirby, *Journal of Geophysical Research: Solid Earth* **88**, B377–B392 (1983).
19. W. Paterson, *Cold Regions Science and Technology* **20**, 75–98 (1991).
20. S. S. Pegler, M. G. Worster, *Journal of fluid mechanics* **696**, 152–174 (2012).
21. W. Budd, *Journal of Glaciology* **9**, 29–48 (1970).
22. D. R. MacAyeal, in *Dynamics of the West Antarctic ice sheet* (Springer, 1987), pp. 141–160.
23. S. S. Pegler, *Journal of Fluid Mechanics* **804**, 24–57 (2016).
24. K. E. Alley *et al.*, *Journal of Glaciology* **64**, 321–332 (2018).
25. A. Tarantola, *Inverse problem theory and methods for model parameter estimation* (siam, 2005), vol. 89.
26. M. G. Wearing, R. C. Hindmarsh, M. G. Worster, *Journal of Glaciology* **61**, 1194–1206 (2015).

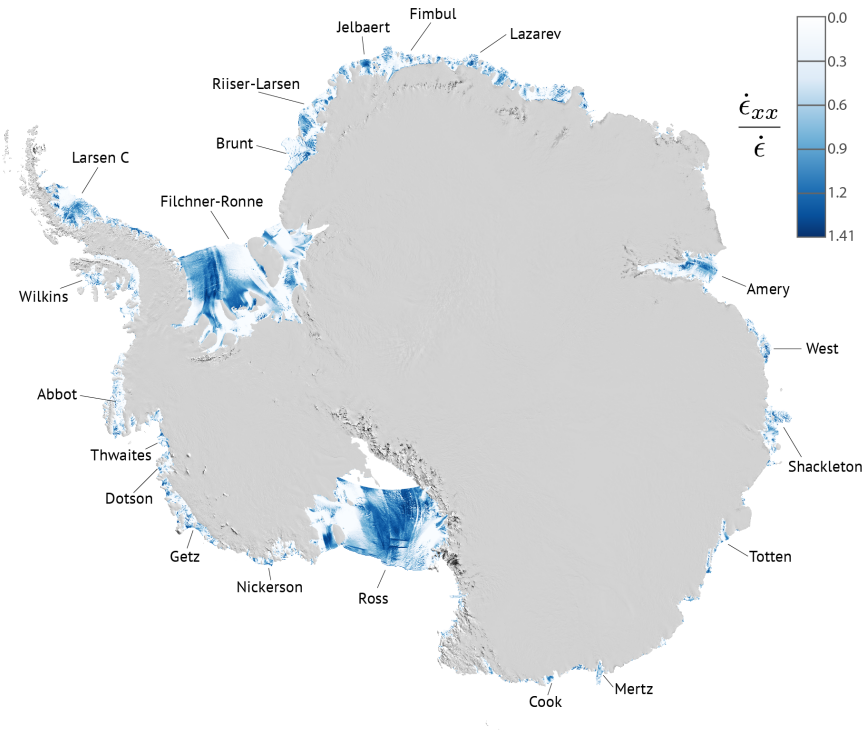

Figure S1: Map of the valid regions used for analysis of the flow law parameters. Grid cells with values < 1.09 were not factored into our work, and as shown in the main text there is no indication that the ratio between the along-flow strain rate and the effective strain rate influences the values of n once they exceed the critical value of 1.0. Cells appropriate for analysis make up approximately 25% of all ice shelf surface area.

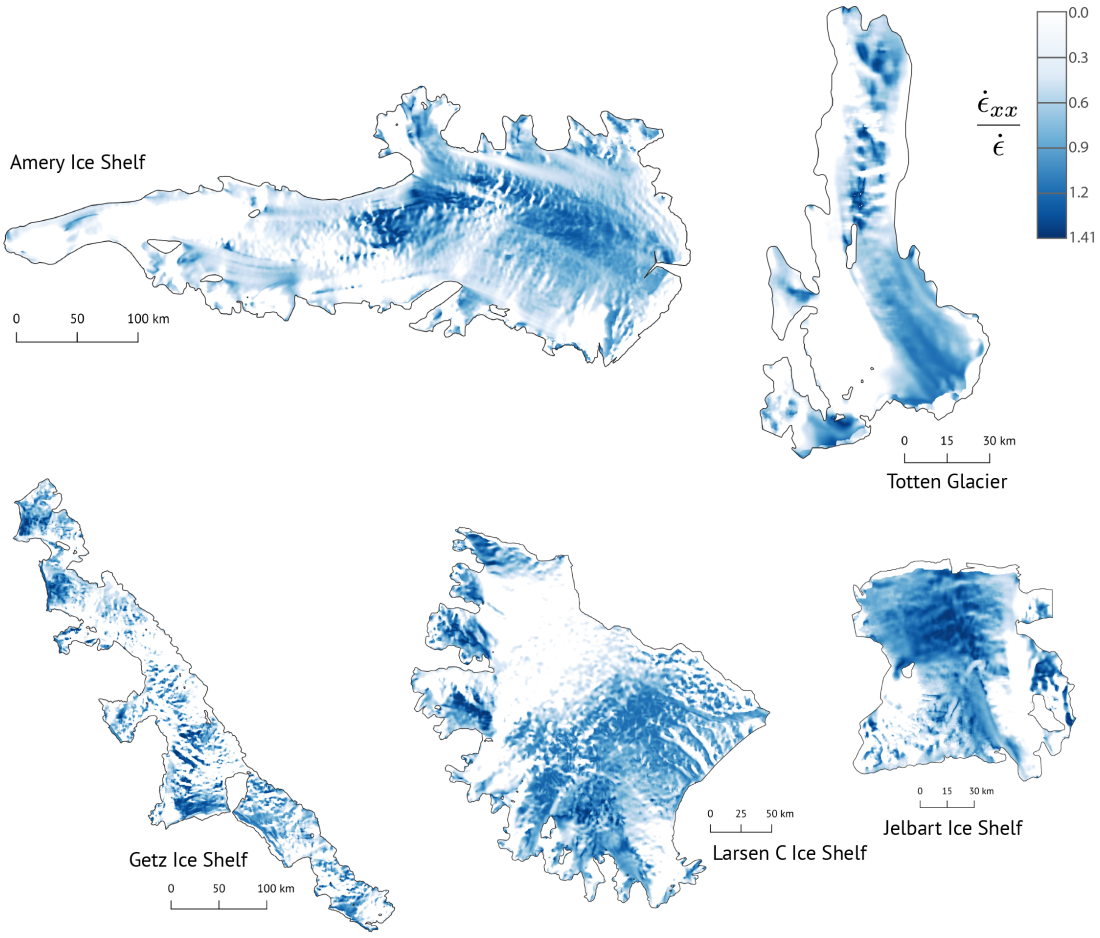

Figure S2: Individual ice shelves across Antarctica illustrating coherent spatial patterns in the ratio between the along-flow strain-rate and the effective strain-rate. We are able to find large swaths of each ice shelf suitable for analysis, even with vastly different oceanic and atmospheric conditions shaping the flow speeds and stress state of the ice shelf.

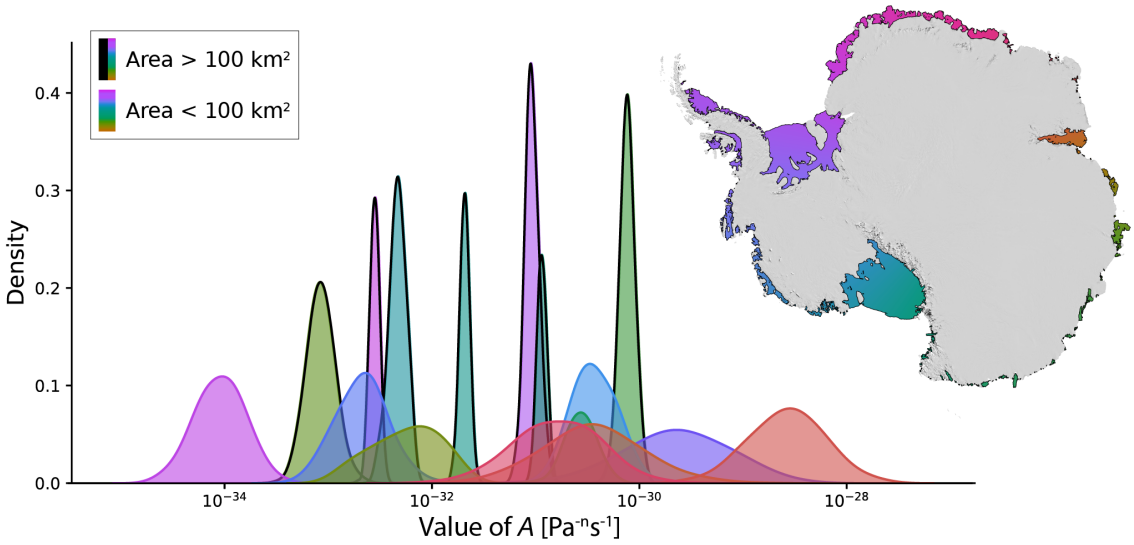

Figure S3: Normalized kernel density estimation of the value of the flow law rate factor, A, obtained over viable regions of Antarctic ice shelves from bootstrap error estimation. The probability density shows that the value of A spans a greater range than the values of n, though a two-order-of-magnitude variability in A is expected from the variability in n and typical stresses ~ 100 kPa. While the size of the areas used for analysis have smaller spread in comparison to smaller geographic areas, the estimates do not center around a single value for A. Rather, results of A match intuition that the values should be smaller than typical values prescribed for $n = 3$, which are on the order of 10^{-25} Pa^{-n} s^{-1}.

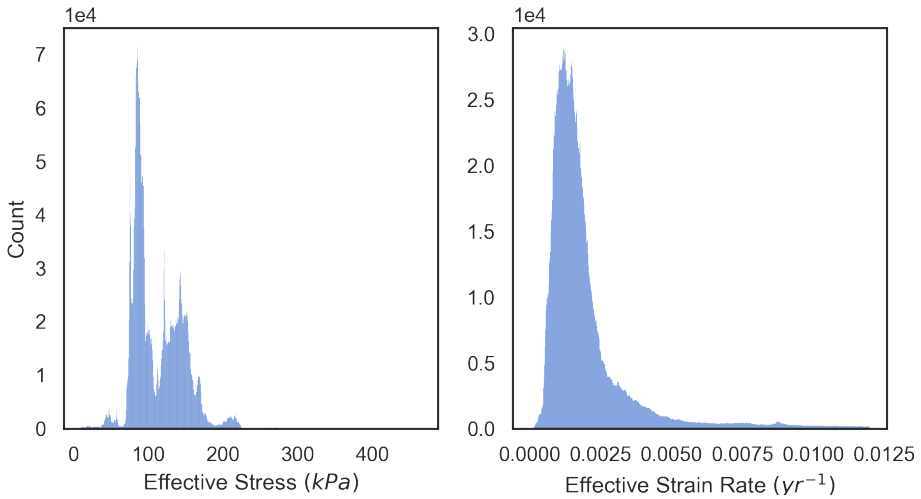

Figure S4: Ranges of the effective deviatoric stress and effective strain rate used for Figures 3 (in the main text) and S3. The values are characteristic of extensional stresses on ice shelves (*11*) and the strain rates are small, indicative of the prosaic deformation in the areas analyzed in this study.